The Astrophysical Journal, 684:1351–1358, 2008 September 10

MULTIWAVELENGTH (RADIO, X-RAY, AND γ-RAY) OBSERVATIONS OF THE γ-RAY BINARY LS I +61 303[1]

J. Albert,[2] E. Aliu,[3] H. Anderhub,[4] P. Antoranz,[5] M. Backes,[6] C. Baixeras,[7] J. A. Barrio,[5] H. Bartko,[8] D. Bastieri,[9]
J. K. Becker,[6] W. Bednarek,[10] K. Berger,[2] C. Bigongiari,[9] A. Biland,[4] R. K. Bock,[8,9] G. Bonnoli,[11] P. Bordas,[12]
V. Bosch-Ramon,[12] T. Bretz,[2] I. Britvitch,[4] M. Camara,[5] E. Carmona,[8] A. Chilingarian,[13] S. Commichau,[4]
J. L. Contreras,[5] J. Cortina,[3] M. T. Costado,[14,15] V. Curtef,[6] F. Dazzi,[9] A. De Angelis,[16] R. de los Reyes,[5]
B. De Lotto,[16] M. De Maria,[16] F. De Sabata,[16] C. Delgado Mendez,[14] D. Dorner,[2] M. Doro,[9] M. Errando,[3]
M. Fagiolini,[11] D. Ferenc,[17] E. Fernández,[3] R. Firpo,[3] M. V. Fonseca,[5] L. Font,[7] N. Galante,[8]
R. J. García López,[1415] M. Garczarczyk,[8] M. Gaug,[14] F. Goebel,[8] M. Hayashida,[8] A. Herrero,[14,15]
D. Höhne,[2] J. Hose,[8] C. C. Hsu,[8] S. Huber,[2] T. Jogler,[8] R. Kosyra,[8] D. Kranich,[4] A. Laille,[17] E. Leonardo,[11]
E. Lindfors,[18] S. Lombardi,[9] F. Longo,[16] M. López,[9] E. Lorenz,[4,8] P. Majumdar,[8] G. Maneva,[19]
N. Mankuzhiyil,[16] K. Mannheim,[2] M. Mariotti,[9] M. Martínez,[3] D. Mazin,[3] C. Merck,[8] M. Meucci,[11]
M. Meyer,[2] J. M. Miranda,[5] R. Mirzoyan,[8] S. Mizobuchi,[8] M. Moles,[20] A. Moralejo,[3] D. Nieto,[5]
K. Nilsson,[18] J. Ninkovic,[8] E. Oña-Wilhelmi,[3] N. Otte,[8,21] I. Oya,[5] M. Panniello,[14,22] R. Paoletti,[11]
J. M. Paredes,[12] M. Pasanen,[18] D. Pascoli,[9] F. Pauss,[4] R. G. Pegna,[11] M. A. Pérez-Torres,[20,23]
M. Persic,[16,24] L. Peruzzo,[9] A. Piccioli,[11] F. Prada,[20] E. Prandini,[9] N. Puchades,[3] A. Raymers,[13]
W. Rhode,[6] M. Ribó,[12] J. Rico,[3,25,23] M. Rissi,[4] A. Robert,[7] S. Rügamer,[2] A. Saggion,[9]
T. Y. Saito,[8] A. Sánchez,[7] M. A. Sánchez-Conde,[20] P. Sartori,[9] V. Scalzotto,[9] V. Scapin,[16]
R. Schmitt,[2] T. Schweizer,[8] M. Shayduk,[8,21] K. Shinozaki,[8] S. N. Shore,[26] N. Sidro,[3]
A. Sillanpää,[18] D. Sobczynska,[10] F. Spanier,[2] A. Stamerra,[11] L. S. Stark,[4] L. Takalo,[18]
P. Temnikov,[19] D. Tescaro,[3] M. Teshima,[8] D. F. Torres,[25,27] N. Turini,[11] H. Vankov,[19]
A. Venturini,[9] V. Vitale,[16] R. M. Wagner,[8] W. Wittek,[8] F. Zandanel,[9]
R. Zanin,[3] and J. Zapatero[7]
(The MAGIC Collaboration)

and

M. A. Guerrero,[20] A. Alberdi,[20] Z. Paragi,[28]
T. W. B. Muxlow,[29] and P. Diamond[29]
Received 2008 January 18; accepted 2008 May 20

ABSTRACT

We present the results of the first multiwavelength observing campaign on the high-mass X-ray binary LS I +61 303, comprising observations at the TeV regime with the MAGIC telescope, along with X-ray observations with *Chandra*, and radio interferometric observations with the MERLIN, EVN, and VLBA arrays, in 2006 October and November. From our MERLIN observations, we can exclude the existence of large-scale (∼100 mas) persistent radio jets. Our 5.0 GHz VLBA observations display morphological similarities to previous 8.4 GHz VLBA observations carried out at the same orbital phase, suggesting a high level of periodicity and stability in the processes behind the radio emission. This makes it unlikely that variability of the radio emission is due to the interaction of an outflow with variable wind clumps. If the radio emission is produced by a milliarcsecond scale jet, it should also show a stable, periodic behavior. It is then difficult to reconcile the absence of a large-scale jet (∼100 mas) in our observations with the evidence of a persistent relativistic jet reported previously. We find a possible hint of temporal correlation between the X-ray and TeV emissions and evidence for radio/TeV noncorrelation, which points to the existence of one population of particles producing the radio emission and a different one producing the X-ray and TeV emissions. Finally, we present a quasi-simultaneous energy spectrum including radio, X-ray, and TeV bands.

Subject headings: gamma rays: observations — X-rays: binaries — X-rays: individual (LS I +61 303)

Online material: color figures

---

[1] Based on observations made with the MAGIC telescope, the *Chandra* X-ray Observatory, and the MERLIN, EVN, and NRAO VLBA arrays.

[2] Universität Würzburg, D-97074 Würzburg, Germany.

[3] IFAE, Edifici Cn., Campus UAB, E-08193 Bellaterra, Spain.

[4] ETH Zurich, CH-8093 Switzerland.

[5] Universidad Complutense, E-28040 Madrid, Spain.

[6] Universität Dortmund, D-44227 Dortmund, Germany.

[7] Universitat Autònoma de Barcelona, E-08193 Bellaterra, Spain.

[8] Max-Planck-Institut für Physik, D-80805 München, Germany.

[9] Università di Padova and INFN, I-35131 Padova, Italy.

[10] University of Łódź, PL-90236 Lodz, Poland.

[11] Università di Siena, and INFN Pisa, I-53100 Siena, Italy.

[12] Universitat de Barcelona, E-08028 Barcelona, Spain.

[13] Yerevan Physics Institute, AM-375036 Yerevan, Armenia.

[14] Instituto de Astrofísica de Canarias, E-38200, La Laguna, Tenerife, Spain.

[15] Depto. de Astrofísica, Universidad, E-38206 La Laguna, Tenerife, Spain.

[16] Università di Udine, and INFN Trieste, I-33100 Udine, Italy.

[17] University of California, Davis, CA-95616-8677.

[18] Tuorla Observatory, Turku University, FI-21500 Piikkiö, Finland.

[19] Institute for Nucl. Research and Nucl. Energy, BG-1784 Sofia, Bulgaria.

[20] Instituto de Astrofísica de Andalucía-CSIC, E-18008 Granada, Spain.

[21] Humboldt-Universität zu Berlin, D-12489 Berlin, Germany.

[22] Deceased.

[23] Corresponding authors: M. A. Pérez-Torres, J. Rico (torres@iaa.es, jrico@icrea.cat).

[24] INAF/Osservatorio Astronomico and INFN, I-34131 Trieste, Italy.

[25] ICREA, E-08010 Barcelona, Spain.

[26] Università di Pisa, and INFN Pisa, I-56126 Pisa, Italy.

[27] Institut de Cienciès de l’Espai (IEEC-CSIC), E-08193 Bellaterra, Spain.

[28] Joint Institute for VLBI in Europe, Dwingeloo, Netherlands.

[29] JBO, University of Manchester, Macclesfield, UK.

1. INTRODUCTION

LS I +61 303 is a high-mass X-ray binary consisting of a low-mass ($M \sim 1$–$4\ M_\odot$) compact object orbiting around an early-type B0 Ve star along an eccentric ($e = 0.7$) orbit (Casares et al. 2005, and references therein). The modulation of both the radio (Gregory & Taylor 1978; Gregory 2002) and X-ray (Taylor et al. 1996; Paredes et al. 1997) emissions display a period of $P_{\rm orb} = 26.496$ days, attributed to the orbital motion. The position of the maximum of the radio emission along the orbit, as well as its intensity, are modulated with a superorbital period of $P_{\rm sup} = 1667 \pm 8$ days (Gregory 2002). LS I +61 303 is positionally coincident with an EGRET γ-ray source (Kniffen et al. 1997). Moreover, variable emission at TeV energies has been recently detected with the MAGIC telescope (Albert et al. 2006a). These authors found that the peak flux at TeV energies occurs at orbital phase $\phi_{\rm orb} \approx 0.65$, while no high-energy emission is detected around periastron passage ($\phi_{\rm orb} \approx 0.23$). From $\sim$50 mas resolution radio images of LS I +61 303 obtained with MERLIN, Massi et al. (2004) suggested the existence of a precessing relativistic ($\beta \approx 0.6$) jet up to angular scales of $\sim 0.1''$, which led them to interpret LS I +61 303 within the framework of the microquasar scenario (Bosch-Ramon et al. 2006; Romero et al. 2007). However, recent VLBA imaging obtained by Dhawan et al. (2006) over a full orbit of LS I +61 303 has shown the radio emission to come from angular scales smaller than about 7 mas (projected size 14 AU at an assumed distance of 2 kpc). This radio emission appeared cometary-like, interpreted to be pointing away from the high-mass star within a particular scenario, and no relativistic motion, nor halos, nor larger scale structures were detected at any phase of the orbit. Based on these findings, Dhawan et al. (2006) concluded that the radio and TeV emissions from LS I +61 303 are originated by the interaction of the wind of a young pulsar with that of the stellar companion (Maraschi & Treves 1981; Dubus 2006).

In this article, we present and discuss the results of a multiwavelength campaign including radio, X-ray, and TeV γ-ray observations of LS I +61 303, with the aim of shedding light on the physical processes going on in the system, as well as yielding useful input for a detailed, time-dependent modeling of this relevant system. For this, we study the correlations between the different detected emissions in terms of their morphological, temporal, and spectral features, at both intraday and day-to-day timescales.

2. MULTIWAVELENGTH OBSERVATIONS

Table 1 and Figure 1 summarize our observations of LS I +61 303, carried out during 2006 October and November. In particular, we set up a simultaneous multiwavelength campaign on LS I +61 303 for 2006 October 25 and 26 using the MERLIN, EVN, and VLBA interferometers (radio), and the TNG (infrared), *Chandra* (X-rays), and MAGIC TeV γ-rays) telescopes. Unfortunately, bad weather conditions did not allow us to get any infrared data, nor did we get useful data from the MAGIC telescope coincident in time with simultaneously scheduled *Chandra* observations. The period November 16–20 included only MAGIC and MERLIN observations.

The range of observed orbital phase in the October campaign was $\phi_{\rm orb} = 0.6$–0.7, for which the TeV maximum has previously been detected (Albert et al. 2006a), and $\phi_{\rm orb} = 0.44$–0.57 in the November campaign. The superorbital phase for both campaigns was $\phi_{\rm sup} = 0.4$.

2.1. *Radio Observations*

We observed LS I +61 303 with several radio interferometric arrays during 2006 October 25–26, including the Multi-Element Radio Linked Interferometer (MERLIN) in the UK, the European VLBI Network (EVN), and the Very Long Baseline Array (VLBA) in the US, all of which observed at 5.0 GHz. In addition, we also monitored the flux and large angular scale structural and flux density variations of LS I +61 303 using MERLIN at 5.0 GHz on 2006 October 27 and 28, and at 6.0 GHz for the period from 2006 November 16 to 20.

TABLE 1

Observing Log for the Multiwavelength Campaign

Telescope	Date	UT range	$\phi_{\rm orb}$[a]	Average Flux[b]
MERLIN	Oct 26	22:32–04:30	0.66	34.84 ± 0.23
	Oct 27	10:30–23:59	0.68	33.74 ± 0.19
	Oct 28	00:00–10:00	0.70	29.63 ± 0.18
	Nov 16	14:43–23:59	0.44	71.41 ± 0.15
	Nov 17	00:00–23:59	0.47	70.78 ± 0.14
	Nov 18	00:00–23:59	0.50	78.98 ± 0.21
	Nov 19	00:00–13:25	0.53	69.05 ± 0.15
	Nov 20	00:00–11:24	0.57	47.14 ± 0.25
EVN	Oct 26	22:30–04:30	0.65	33.29 ± 0.27
VLBA	Oct 25	21:30–02:50	0.61	39.49 ± 0.18
	Oct 26	21:30–02:50	0.65	32.69 ± 0.14
Chandra	Oct 25	22:13–04:26	0.61	1.87 ± 0.16
MAGIC	Oct 27	00:50–04:29	0.66	1.7 ± 0.4
	Nov 16	21:33–01:04	0.45	<1.19
	Nov 17	20:56–01:00	0.48	<0.80
	Nov 18	21:00–22:19	0.52	<1.51
	Nov 19	21:00–22:00	0.56	<1.31

[a] The orbital and superorbital phases are computed using $\mathrm{MJD}_0 = 43366.275$, $P_{\rm orb} = 26.4960$ (Gregory 2002). The superorbital phase is $\phi_{\rm sup} = 0.4$ for the whole observation period.

[b] The average measured fluxes are in mJy for radio observations (MERLIN, EVN, VLBA), 10^{-11} ergs cm^{-2} s^{-1} for the *Chandra* X-ray observations (absorbed power-law), and 10^{-11} photons cm^{-2} s^{-1} for the MAGIC VHE γ-ray observations. Upper limits are given at the 95% confidence level, following the prescription by Rolke et al. (2005). The data were taken at 5.0 GHz for the radio observations (except for the MERLIN data in 2006 November, which were taken at 6.0 GHz), at 0.5–10 keV by *Chandra*, and at 0.3–5.0 TeV by MAGIC.

The MERLIN array included six antennas (Defford, Cambridge, Knockin, Darnhall, Jodrell Bank [Mk II], and Tabley) for most of our observations, yielding synthesized beams of about 50–70 mas (corresponding to projected linear sizes of 100–140 AU). The EVN observations on 2006 October 26, which were the first ever carried out for LS I +61 303 using the e-VLBI technique (Szomoru et al. 2006), included five antennas spread over Europe (Cambridge, Jodrell Bank Mk II, Medicina, Torun, and the Westerbork phased array), yielding a synthesized beam of about 7 mas (or 14 projected AU). The data were directly streamed to the correlator at JIVE (Joint Institute for VLBI in Europe, Dwingeloo, The Netherlands) through the Internet; this was one of the first science observations that achieved 256 Mbps sustained data rate with the e-VLBI technique. The VLBA observations on 2006 October 25 and 26 included ten 25 m antennas spread over the US, yielding a beam size of 4.6 × 2.1 mas, corresponding to a projected linear resolution of $\sim$9.2 AU and $\sim$4.2 AU in right ascension and declination, respectively.

All three interferometric arrays observed LS I +61 303 in phase-referenced mode. LS I +61 303 and the bright ($S_{\rm 5GHz} \approx 600$ mJy), nearby International Celestial Reference Frame (ICRF) source J0244+6228 were alternately observed through each observing run, the phases of J0244+6228 being transferred to the position of LS I +61 303 in the post-observation data analysis. J0244+6228 also served as amplitude calibrator for our observations. We performed standard calibration and data reduction within the NRAO Astronomical Imaging Package System (AIPS;

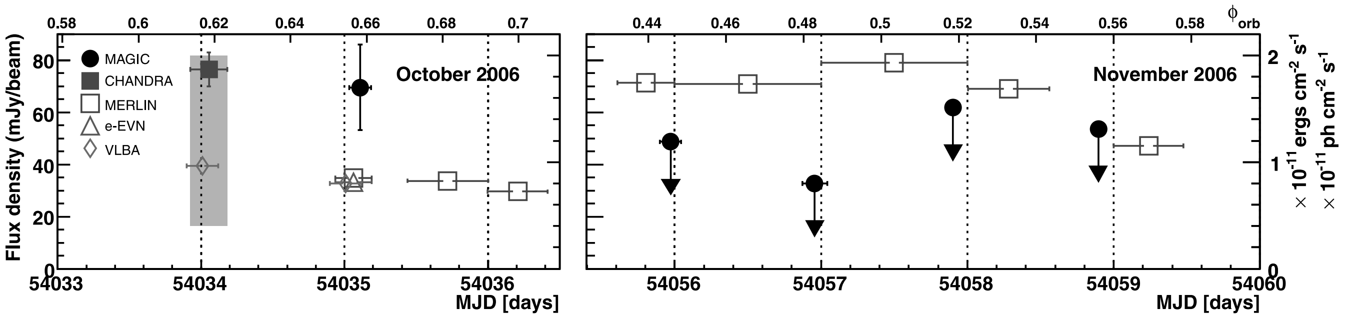

FIG. 1.—Radio, X-ray, and VHE γ-ray light curves obtained with VLBA, EVN, MERLIN (left-hand scale), *Chandra* (right-hand scale, in 10^{-11} ergs cm^{-2} s^{-1}), and MAGIC (right-hand scale in 10^{-11} photons cm^{-2} s^{-1}) during the two observing periods (2006 October and November). The horizontal error bars show the time spanned by the different observations. The shaded area marks the range of X-ray flux values previously reported (see Table 3). The upper axis shows the orbital phase using the ephemeris from Gregory (2002). [*See the electronic edition of the Journal for a color version of this figure.*]

Diamond 1995). We also used standard hybrid mapping techniques within AIPS to obtain the flux densities shown in Figure 1 and Table 1, and the radio images shown in Figures 2 and 3

2.2. *X-Ray Observations*

We obtained *Chandra* X-ray observations of LS I +61 303 on 2006 October 25 through the Director Discretionary Time program (*Chandra* ObsId 8273). The observations were carried out using ACIS-I for a total exposure time of 20.0 ks. At the time of the observation, LS I +61 303 was expected to be in a high state, and its high X-ray brightness could have resulted in an excessively high count rate, producing appreciable pile-up in the observations. In order to minimize pile-up effects, LS I +61 303 was offset by 8′ from the ACIS-I aim point, thus smearing its image and reducing the count rate at the source peak. We further used 1/4 subarray, reducing the exposure time of individual frames from the nominal exposure time of 3.2 s down to 0.8 s.

Data reduction of the X-ray observations of LS I +61 303 has been performed using the *Chandra* X-ray Center software CIAO V3.4. The data reduction included the application of standard filters and rejection of events with bad grades and those originating from bad pixels. The background count rate is consistent with the quiescent background (Markevitch 2001), and no time intervals of enhanced background needed to be removed. The processed observations have a useful exposure time of 19.1 ks. Due to the high count rate of LS I +61 303, out-of-time events were not negligible and produced a noticeable streak along the columns. These have been corrected using the CIAO task `acisreadcorr`. Finally, we note that as of CALDB v3.1.0 (2005 June), the CIAO task `acis_process_events` is routinely used by the level 1 processing pipeline to mitigate the charge transfer inefficiency (CTI) that affects the *Chandra* ACIS-I front-illuminated chips. Therefore, no further CTI correction was applied. Light curves and spectra of LS I +61 303 were obtained using standard CIAO tasks and analyzed using HEASARC FTOOLS and XSPEC v11.2.0 routines (Arnaud 1996).

2.3. *VHE γ-Ray Observations*

Observations in the very high energy (VHE) γ-ray band ($E_\gamma >$ 100 GeV) were scheduled with the MAGIC telescope on 2006 October 26–28 and November 16–19 (see Table 1). These observations are part of an extensive, stand-alone observing campaign carried out between 2006 September and December (J. Albert et al. 2008, in preparation). Bad weather conditions at the Observatorio del Roque de los Muchachos, however, prevented us from obtaining useful data on 2006 October 26 and 28.

The observations were carried out in the false-source track (wobble) mode (Fomin et al. 1994), with two directions at 24′ distance and opposite sides of the source direction, which allows for a reliable estimation of the background with no need for extra observation time.

The data were analyzed using the standard MAGIC calibration and analysis software (Albert et al. 2006b; Gaug et al. 2005). Data runs with anomalous event rates were discarded from further analysis. Hillas variables (Hillas 1985) were combined into an adimensional γ/hadron discriminator (“hadronness”) and an

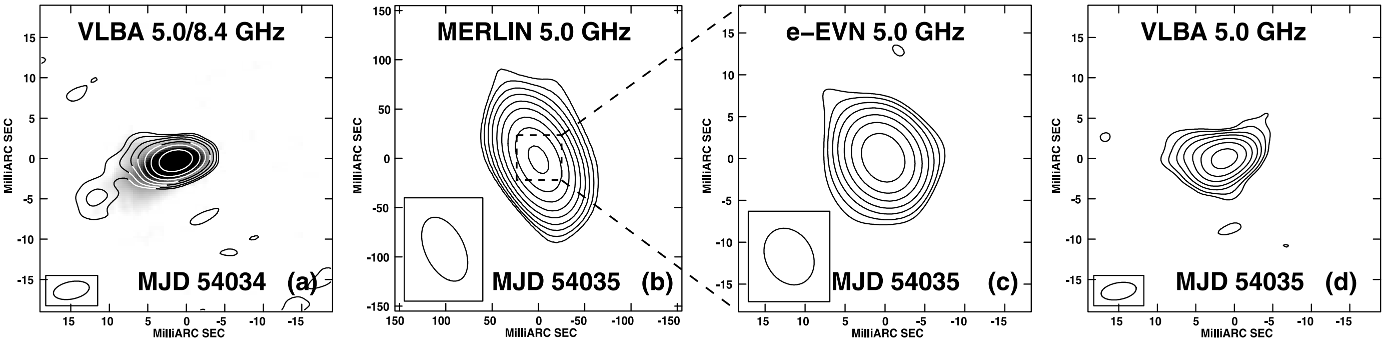

FIG. 2.—Radio images of LS I +61 303 obtained (*a*) on 2006 October 25 with the VLBA, and on 2006 October 26 with (*b*) MERLIN, (*c*) EVN, and (*d*) VLBA. The synthesized beams of the images (bottom left corner in each panel) are 70 × 41 mas (position angle PA = 29°), 7.2 × 5.8 mas (PA = 35°), and 4.6 × 2.1 mas (PA = −81°) for the MERLIN, EVN, and VLBA observations, respectively. The projected linear resolution of our VLBA observations is thus 9.2 and 4.2 AU in R.A. and decl., respectively. In (*a*) we also show overlaid the 8 GHz VLBA image on 2006 February 2 (*gray scale*), convolved with our 5 GHz VLBA beam. This date corresponds to the same phase of LS I +61 303 ($\phi_{\rm orb} \approx 0.62$), and they show a striking similarity. In all cases, the origin of coordinates is set at the VLBA peak of brightness on 2006 October 25, and the contours are drawn at (3, $3\sqrt{3}$, 9, ...) times the off-source rms (see Table 1).

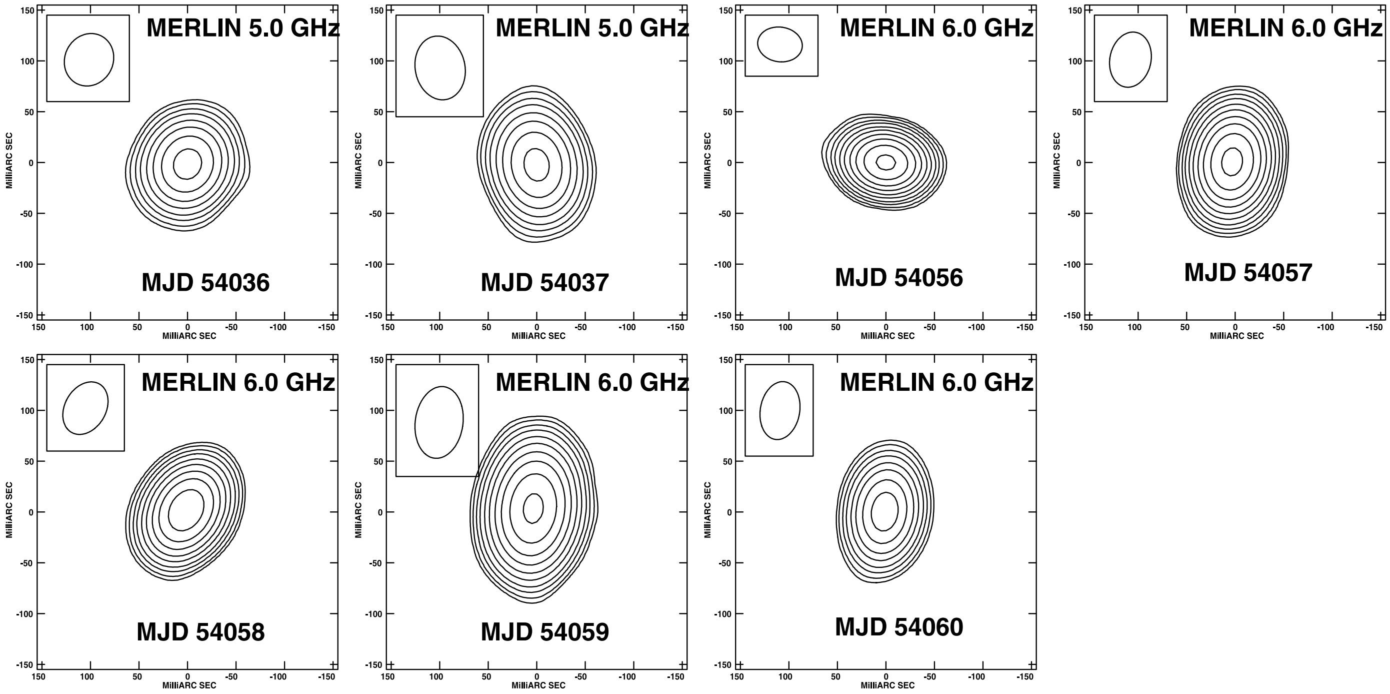

Fig. 3.—Radio images of LS I +61 303 obtained with MERLIN during our 2006 October and November campaigns. The images correspond, from left to right and top to bottom, to observations carried out on 2006 October 27 and 28 at a frequency of 5.0 GHz, and on 2006 November 16, 17, 18, 19, and 20 at a frequency of 6.0 GHz. Radio contours are drawn at $(3, 3\sqrt{3}, 9, \ldots)$ times the off-source rms (see Table 1). Note that the shape of the radio brightness distribution of LS I +61 303 genuinely follows the synthesized beam for each epoch (upper left inset in each panel).

energy estimator by means of the random forest classification algorithm, which takes into account the correlation between the different Hillas variables (Breiman 2001; Bock et al. 2005). The incoming direction of the primary γ-ray events was estimated using the DISP method, suited for observations with a single IACT (Fomin et al. 1994; Domingo-Santamaría et al. 2005).

3. RESULTS

In this section we present the results obtained from the different multiwavelength observations we have performed, and put them into the context of the past measurements in the different bands. They are summarized in Table 1 and Figure 1.

3.1. *Radio Results*

The total radio flux density obtained with MERLIN shows a decline between October 26 ($\phi_{\rm orb} = 0.66$) and October 28 ($\phi_{\rm orb} = 0.70$), from ~35 to ~30 mJy, and a peak on 18 November ($\phi_{\rm orb} = 0.50$) at ~80 mJy. At the superorbital phase of the observations ($\phi_{\rm sup} = 0.4$), the radio source is in the weak state. The predicted flux of the radio flux is between 50 and 100 mJy at the orbital phases $\phi_{\rm orb} \sim 0.9$. We therefore measure a flux compatible with the predicted one, although at a much earlier phase value. However, for the weak state, secondary peaks of comparable flux show up at other orbital phase values (see, e.g., Dhawan et al. 2006).

In Figure 2 we show the radio images corresponding to October 25–26, where all three arrays observed simultaneously LS I +61 303. In Figure 3 we show the MERLIN images obtained on 2006 October 27 and 28 at 5.0 GHz, and on November 16–20 at 6.0 GHz. Our MERLIN observations show no evidence for large angular scale structures, contrary to what had been previously claimed (Massi et al. 2004), hence excluding the existence of persistent jets at these scales. The structure of LS I +61 303 genuinely follows the beam shape of the MERLIN array at all epochs. Model fits to the *u*-*v* plane of the MERLIN data show that the projected intrinsic size of the radio-emitting region of LS I +61 303 is, at any observing epoch, no larger than ~6 mas (~12 AU), as confirmed by our higher resolution images obtained with the EVN and the VLBA.

Our 5 GHz VLBA images on 25 and 26 October show a very bright and unresolved component, plus an extended radio emission to the east-southeast (see Fig. 2). The general aspect of the radio emission recalls the structure found by Dhawan et al. (2006). Figure 2*a* shows both, with our 5 GHz VLBA image on 2006 October 25 ($\phi_{\rm orb} = 0.62$, contours) overlaid on top of the 8.4 GHz VLBA data from 2006 February 2 ($\phi_{\rm orb} = 0.62$, gray scale), kindly provided by V. Dhawan in advance of publication.

The projected distance from the peak of the radio brightness distribution to the edge of the extended region is, as imaged with the VLBA at 5.0 GHz on 2006 October 26, about ~8.2 mas (16.4 AU). If the maximum time to fill in this region with radio (synchrotron) emitting particles is less that the time spanned by our two consecutive VLBA observations (1 day), the implied outflow velocity is at least of 21,500 km $\rm s^{-1}$, or $v \gtrsim 0.09\ c$.

The coordinates of the peak of radio brightness distribution of LS I +61 303, as obtained from our VLBA observations (using task IMFIT), were R.A. = $02^{\rm h}40^{\rm m}31.6638849^{\rm s}$, decl. = $61°13'45.592235''$ on October 25, and R.A. = $02^{\rm h}40^{\rm m}31.6638756^{\rm s}$, decl. = $61°13'45.592496''$ on October 26, with and estimated accuracy of 12 μas and 7 μas in R.A. and decl., respectively. This shift of the brightness peak corresponds to a day-to-day projected speed of 904 ± 60 km $\rm s^{-1}$, in excellent agreement with the typical value of ~1000 km $\rm s^{-1}$ found by Dhawan et al. (2006) along a complete orbital cycle.

The peak flux density varied significantly between our two VLBA observing runs, decreasing from 24.3 mJy $\rm beam^{-1}$ on October 25 to 15.4 mJy $\rm beam^{-1}$ on October 26. The total 5 GHz flux density varied from 39.5 ± 0.2 mJy [radio luminosity $L_R = (9.5 \pm 0.1) \times 10^{29}$ ergs $\rm s^{-1}$] to 32.7 ± 0.2 mJy [$L_R = (7.8 \pm 0.1) \times 10^{29}$ ergs $\rm s^{-1}$].

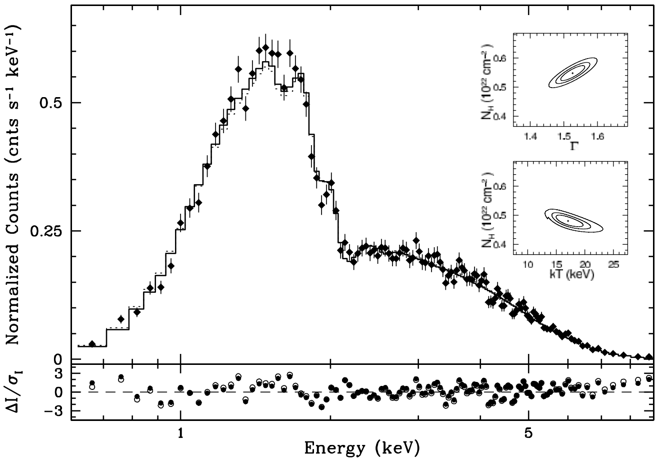

FIG. 4.—*Chandra* ACIS-I spectrum of LS I +61 303 overplotted with the best-fit absorbed power-law (*solid histogram*) and bremsstrahlung (*dotted histogram*) models (see Table 3 for details). The lower panel shows the relative residuals of the fits (ΔI) in terms of the bin standard deviation (σ) for both the absorbed power-law (*filled circles*) and bremsstrahlung (*open circles*) models. The errors bars in both the spectra and residual plots are 1 σ. The insets show the χ^2 plots as a function of the power-law index, Γ, and $N_{\rm H}$ (*upper inset*), and of the plasma temperature, *kT*, and $N_{\rm H}$ (*lower inset*) of the spectral fits to the *Chandra* ACIS-I spectrum of LS I +61 303 using absorbed power-law and bremsstrahlung models, respectively. The contours represent 68%, 90%, and 99% confidence levels. [*See the electronic edition of the Journal for a color version of this figure.*]

We therefore suggest that the drop seen in the total radio flux density of LS I +61 303 between our two consecutive VLBA observations is directly related to the change in the peak flux density, which hints toward a physical link with structural variations in the innermost ($\lesssim$3 mas projected radius, or 6 AU at a distance of 2 kpc) region of the source, which our observations cannot resolve.

3.2. *X-Ray Results*

LS I +61 303 is clearly detected in our *Chandra* observation, with a background-subtracted averaged count rate of 1.067 ± 0.008 counts s^{-1} in the energy band 0.5–10.0 keV. This count rate would have indeed resulted in considerable pile-up for a standard observational setup. The X-ray spectrum (Fig. 4) shows a broad peak at ~1.6 keV and a hard energy tail that extends up to 9 keV. Assuming a foreground interstellar absorption with solar abundances and the absorption cross sections of Balucinska-Church & McCammon (1992), the X-ray spectrum of LS I +61 303 can be reasonably well fitted by either an absorbed power law, or an absorbed bremsstrahlung model (Fig. 4). The best-fit parameters, goodness of the fit (reduced χ^2), and implied source flux and luminosity in the energy range of 0.5–10.0 keV for these two models are listed in Table 2. In both cases, the unabsorbed X-ray luminosity of LS I +61 303 in the energy range of 0.5–10.0 keV is $\sim 10^{34}$ ergs s^{-1}.

TABLE 2

X-RAY SPECTRUM BEST-FIT PARAMETERS

Parameter	Power-Law	Bremsstrahlung
χ^2/dof..............................	413.95/370 = 1.12	428.24/370 = 1.16
$N_{\rm H}$ (10^{21} cm^{-2})................	5.5 ± 0.5	4.8 ± 0.4
Γ or *kT*............................	1.53 ± 0.07	17^{+6}_{-4} keV
$f_{\rm obs}^{0.5-10.0\ {\rm keV}}$	1.87 ± 0.16	1.84 ± 0.05
$L^{0.5-10.0\ {\rm keV}}$	1.18 ± 0.11	1.11 ± 0.04

NOTES.—Best-fit parameters to the X-ray spectrum for LS I +61 303 obtained using absorbed power-law and bremsstrahlung models. The flux between 0.5 and 10.0 keV is expressed in 10^{-11} ergs cm^{-2} s^{-1}, and the luminosity in 10^{34} ergs s^{-1} and for an assumed distance of 2 kpc.

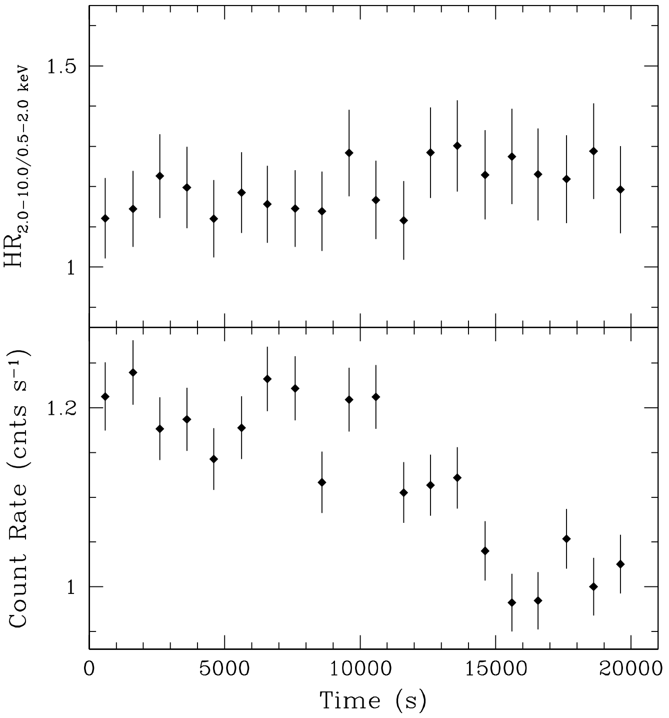

FIG. 5.—Temporal evolution of the *Chandra* ACIS-I hardness ratio (*top*) and count rate in the energy band 0.5–10.0 keV (*bottom*). The bin size is 1000 s, and the error bars are 1 σ.

We have also investigated the short-term variability of LS I +61 303 X-ray flux and hardness ratio (defined as the ratio of the count rate between 2.0 and 10.0 keV over that between 0.5 and 2.0 keV), shown in Figure 5. The *Chandra* ACIS-I count rate of LS I +61 303 in the energy band of 0.5–10.0 keV varied by a factor of 25%, from $\sim 1.25 \pm 0.03$ counts s^{-1} down to $\sim 1.00 \pm 0.03$ counts s^{-1}, within a timescale of 1–2 hr, showing a clear decline in the final third of the observation. The probability that this variation is a statistical fluctuation of a constant flux is less than 10^{-15}, as obtained from a χ^2 fit of a constant function to the data set. Fast flux variations of up to 70% within few hours timescale have been reported by Sidoli et al. (2006). In their case, these were accompanied by variations in the hardness ratio (HR = 2–12 keV/0.3–2 keV) of about 30%, which our data do not confirm. It must be noted, however, that assuming a linear correlation between flux and HR, we should observe less than ~10% variations in the HR during our observation, which is below our statistical error.

Table 3 summarizes the results of the observations of LS I +61 303 in the ~1–10 keV energy range existing in the literature, including that obtained in our *Chandra* observations. We measure a flux of 1.9×10^{-11} ergs cm^{-2} s^{-1} and a photon index 1.53. The historical values obtained over several years range between $[0.4-2.0] \times 10^{-11}$ ergs cm^{-2} s^{-1} for the flux and [1.25–1.83] for the photon index. Therefore, we observed the source in a particularly high and hard state. This is shown also in Figure 6, where we plot the historical values of the photon index against the flux, in the soft X-ray range. The Pearson's correlation coefficient between these two quantities is $r = -0.46$, but becomes $r = -0.91$ when the outlier point obtained by Paredes et al. (2007) is removed from the computation. This is, to our knowledge, the first time that this correlation is shown, and confirms the claim by Sidoli et al. (2006) that the source is harder when it is brighter.

TABLE 3
X-Ray Observations of LS I +61 303 in the ~1–10 keV Range

ObsID	Date	Exposure	$\phi_{\rm orb}$	$\phi_{\rm sup}$	Γ	f
A0	1994 Feb 03	18.0	0.20	0.61	1.71 ± 0.08	0.72
A1	1994 Feb 09	19.3	0.43	0.61	1.83 ± 0.08	0.52
R0	1996 Mar 01	8.9	0.79	0.07	...	0.84
R1	1996 Mar 04	9.3	0.91	0.07	...	1.21
R2	1996 Mar 07	9.4	0.03	0.07	...	0.69
R3	1996 Mar 10	9.1	0.11	0.07	...	0.65
R4	1996 Mar 13	10.0	0.22	0.07	...	0.96
R5	1996 Mar 16	9.5	0.33	0.07	...	1.32
R6	1996 Mar 18	9.5	0.42	0.08	...	2.00
R7	1996 Mar 24	11.0	0.64	0.08	...	1.22
R8	1996 Mar 26	13.7	0.71	0.08	...	1.03
R9	1996 Mar 30	14.6	0.87	0.08	...	0.92
S0	1997 Sep 22	12.0	0.31	0.41	1.68 ± 0.16	0.48 ± 0.01
S1	1997 Sep 26	8.6	0.45	0.41	1.56 ± 0.09	1.40 ± 0.01
X0	2002 Feb 05	6.4	0.56	0.37	1.60 ± 0.02	1.39 ± 0.01
X1	2002 Feb 10	6.4	0.76	0.37	1.53 ± 0.02	1.35 ± 0.01
X2	2002 Feb 17	6.4	0.01	0.37	1.74 ± 0.05	0.50 ± 0.01
X3	2002 Feb 21	7.5	0.18	0.38	1.57 ± 0.02	1.36 ± 0.01
X4	2002 Sep 16	6.4	0.97	0.50	1.60 ± 0.07	1.39 ± 0.01
X5	2005 Jan 27	48.7	0.60	0.02	1.62 ± 0.01	1.29 ± 0.01
					1.83 ± 0.01	0.40 ± 0.01
C0	2006 Apr 07	49.9	0.03	0.28	1.25 ± 0.09	0.71 ± 0.18
C1	2006 Oct 25	20.0	0.61	0.40	1.53 ± 0.07	1.87 ± 0.02

Notes.—The first column shows an ID composed of a letter standing for the X-ray satellite: A = *ASCA* (Leahy et al. 1997), R = *RXTE* (Harrison et al. 2000), S = *BeppoSAX* (Sidoli et al. 2006), X = *XMM-Newton* (Sidoli et al. 2006; Chernyakova et al. 2006), C = *Chandra* (Paredes et al. 2007 and this work), and an ordering index. Observation C1 corresponds to the one performed during our multiwavelength campaign. The exposure is in ks. The terms $\phi_{\rm orb}$ and $\phi_{\rm sup}$ are the orbital and superorbital phases of the beginning of the observation, computed using $T_0 = 43366.275$, $P_{\rm orb} = 26.4960$ days, and $P_{\rm sup} = 1667$ days (Gregory 2002). The photon index (Γ) is obtained from a fit to an absorbed power-law model. The flux (f) is expressed in 10^{-11} ergs cm^{-2} s^{-1}, and is integrated between 2 and 10 keV for *RXTE*, *BeppoSAX*, and *XMM-Newton*, between 0.3 and 10 keV for observation C0, and between 0.5 and 10 keV for C1.

3.3. *VHE γ-Ray Results*

LS I +61 303 was detected with MAGIC only on October 27 ($\phi_{\rm orb} = 0.66$), with a significance of 4.5 σ. For the rest of the nights, no detection above 2 σ was found, and we derived the corresponding upper limits to the integral flux (see Table 1).

On October 27, the measured average flux above 300 GeV corresponds to 15% of the Crab Nebula flux at these energies. The VHE γ-ray source is pointlike for the MAGIC angular resolution (0.1°), and the location is compatible with that of LS I +61 303. The energy spectrum is well fitted by an unbroken power-law with index $\alpha = -2.7 \pm 0.5 \pm 0.2$, where the quoted errors correspond to the statistical and systematic uncertainties, respectively. No significant variations of the absolute flux were detected within that night.

Previous observations of this source with the MAGIC (Albert et al. 2006a, 2008) and VERITAS (Acciari et al. 2008) telescopes have shown a pointlike source, with a peak of ~15% Crab flux intensity at orbital phase $\phi_{\rm orb} \sim 0.65$, and a spectral index $\alpha \sim -2.6$, hence in agreement with the results derived from our observations.

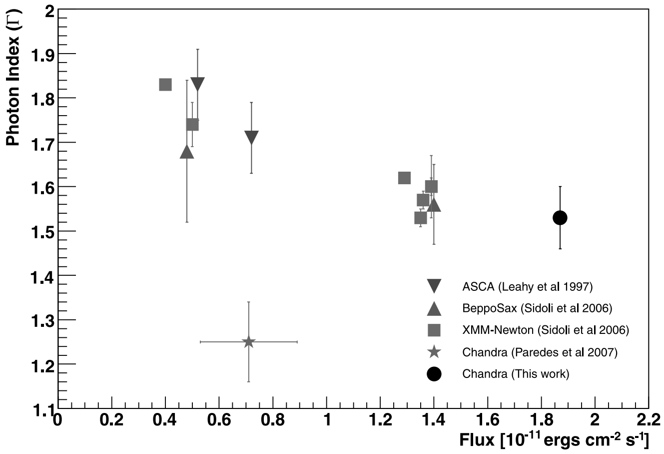

Fig. 6.—Correlation between the X-ray flux and photon index for the existing observations of LS I +61 303 in the ~1–10 keV energy band, obtained by using public data from the literature and our own data. (See main text for details). [*See the electronic edition of the Journal for a color version of this figure.*]

4. DISCUSSION

The comparison between VHE γ-ray and radio data during the October campaign (see Fig. 1) shows a detection at TeV energies for $\phi_{\rm orb} = 0.66$ with a flux level of ~15% of the Crab Nebula flux, during a period when the radio emission is constant at 35 mJy. During the November campaign, however, there is no detection at TeV energies, while the radio data show a peak flux twice as high as in October. Albert et al. (2006a) reported radio and TeV peaks detected almost simultaneously, while for our campaign we see the TeV peak for a flat and low radio flux and a radio peak for no significant TeV emission. Therefore, we exclude a general TeV-radio correlation. A plausible explanation is that the emissions are produced by different particle populations. On the other hand, the detections at X-ray and TeV energies, both at particularly

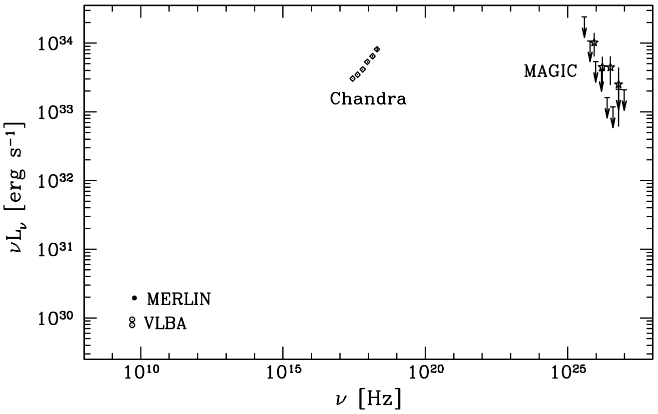

FIG. 7.— Quasi-simultaneous LS I +61 303 spectrum including radio (VLBA; *open circles*), X-rays (*Chandra*; *squares*) and VHE γ-rays (MAGIC; *stars*) data from the period 2006 October 25–26, along with the data from 2006 November: average MERLIN flux density (*filled circle*) and upper limits from MAGIC (*arrows*).

high flux values and 1 day apart, might point to a correlation between X-ray and TeV fluxes, and hence to the fact that both radiations are produced by the same population of particles. However, our data are too scarce to make any definite conclusion at present.

The results obtained by radio imaging at different angular scales show that the size of the radio emitting region of LS I +61 303 is constrained below $\sim$6 mas ($\sim$12 projected AU), and the presence of persistent jets above this scale is therefore excluded.

We resolve a radio-emitting region at 5.0 GHz with the VLBA, extending east-southeast from the brighter, unresolved emitting core. The outflow velocity implied by our observations is at least of $\sim$0.1 *c*, in agreement to what was previously suggested by Chernyakova et al. (2006) for an overpressured pulsar wind, although recent hydrodynamical simulations (Bogovalov et al. 2008) show that the shocked pulsar wind could be relativistic.

The comparison of our VLBA image from 25 October with an image at 8.4 GHz obtained at a similar orbital phase, but 10 orbital cycles apart, shows a high level of similarity between them. It is worth noting that Dhawan et al. (2006) obtained high-resolution radio images of the source along a complete orbital cycle, and found an extended feature whose orientation with respect to the central core varied by 360° along the orbit. Therefore, the similarity in the morphology and orientation between the two images suggests a significant level of periodicity and stability of the physical processes involved in the radio emission. This result points to the fact that the extended radio emission is produced by the interaction of steady flows (from a relativistic pulsar wind, jet and/or stellar wind) rather than by the interaction of such an outflow with wind clumps. We note that if the radio emission is produced by a milliarcsecond scale jet, the required stability and periodic behavior of such a jet is difficult to reconcile with the nonpersistent nature of a large-scale ($\sim$100 mas), putative relativistic jet, as deduced from our MERLIN observations in combination with those obtained by Massi et al. (2004).

Finally, we combine our X-ray data from 25 October, the TeV data from 26 October, and the average VLBA in both nights to produce a quasi-simultaneous multiwavelength spectrum, including radio, X-ray, and VHE γ-ray observations, which we display in Figure 7. However, the simultaneous data cover only a small range of the orbital phase of LS I +61 303. Given the high variability of the physical conditions of the system along the orbit, more simultaneous multiwavelength data, and particularly involving longer exposure times, orbital phase coverage, and redundancy, will shed further light in our understanding of this peculiar object.

We thank the IAC for the excellent working conditions at the ORM. We also thank the support given by the *Chandra* telescope and the MERLIN interferometer through their Discretionary Director Time programs, as well as the observing time provided by the e-EVN, and the NRAO VLA and VLBA interferometers via Target of Opportunity proposals. We are grateful to the anonymous referee for the useful comments and suggestions which have improved this paper greatly. The support of the German BMBF and MPG, the Italian INFN, the Spanish MEC, the ETH Research Grant TH 34/04 3 and the Polish MNiI Grant 1P03D01028 is gratefully acknowledged. This research is partially supported by the Ramón y Cajal programme of the Spanish MEC. The European VLBI Network (EVN) is a joint facility of European, Chinese, South African and other radio astronomy institutes funded by their national research councils. e-VLBI developments in Europe are supported by EC DG-INFSO funded Communication Network Development project, EXPReS, contract 02662. MERLIN is a National Facility operated by the University of Manchester at Jodrell Bank Observatory on behalf of STFC. This work has benefited from research funding from the European Community's sixth Framework Programme under RadioNet R113CT 2003 5058187. The National Radio Astronomy Observatory is a facility of the National Science Foundation operated under cooperative agreement by Associated Universities, Inc.

REFERENCES

Acciari, V. A., et al. 2008, ApJ, in press
Albert, J., et al. 2006a, Science, 312, 1771
———. 2006b, preprint (astro-ph/0612385)
———. 2008, ApJ, submitted (arXiv:0806.1865)
Arnaud, K. A. 1996, in ASP Conf. Ser. 101, Astronomical Data Analysis Software and Systems V, ed. G. H. Jacoby & J. Barnes (San Francisco: ASP), 17
Balucinska-Church, M., & McCammon, D. 1992, ApJ, 400, 699
Bock, R. K., et al. 2005, Nucl. Instrum. Method. A, 516, 188
Bogovalov, S. V., et al. 2008, MNRAS, 387, 63
Bosch-Ramon, V., Paredes, J. M., Romero, G. E., & Ribó, M. 2006, A&A, 459, L25
Breiman, L. 2001, Machine Learning, 45, 5
Casares, J., Ribas, I., Paredes, J. M., Martí, J., & Allende Prieto, C. 2005, MNRAS, 360, 1105
Chernyakova, M., Neronov, A., & Walter, R. 2006, MNRAS, 372, 1585
Dhawan, V., Mioduszewski, A., & Rupen, M. 2006, Proc. VI Microquasar Workshop, ed. T. Belloni (Como: Proceedings of Science), 52.1
Diamond, P. J. 1995, in ASP Conf. Ser. 82, Very Long Baseline Interferometry and the VLBA, ed. J. A. Zensus, P. J. Diamond, & P. J. Napier (San Francsico: ASP), 227
Domingo-Santamaría, E., et al. 2005, Proc. 29th Int. Cosmic Ray Conf. (Pune, India), 5, 363
Dubus, G. 2006, A&A, 456, 801
Fomin, V. P., Stepanian, A. A., Lamb, R. C., Lewis, D. A., Punch, M., & Weekes, T. C. 1994, At. Phys., 2, 137
Gaug, M., et al. 2005, Proc. 29th Int. Cosmic Ray Conf. (Pune, India), 5, 375
Gregory, P. C. 2002, ApJ, 575, 427
Gregory, P. C., & Taylor, A. R. 1978, Nature, 272, 704
Harrison, F. A., et al. 2000, ApJ, 528, 454
Hillas, A. M. 1985, Proc. 19th Int. Cosmic Ray Conf. (La Jolla), 3, 445
Kniffen, D. A., et al. 1997, ApJ, 486, 126
Leahy, D. A., Harrison, F. A, & Yoshida, A. 1997, ApJ, 475, 823
Maraschi, L., & Treves, A. 1981, MNRAS, 194, 1P
Markevitch, M. 2001, ACIS Background (Cambridge: CXC), http://cxc.harvard.edu/contrib/maxim/bg/index.html
Massi, M., Ribó, M., Paredes, J. M., Garrington, S. T., Peracaula, M., & Martí, J. 2004, A&A, 414, L1
Paredes, J. M., Marti, J., Peracaula, M., & Ribo, M. 1997, A&A, 320, L25

Paredes, J. M., Ribó, M., Bosch-Ramon, V., West, J. R., Butt, Y. M., Torres, D. F., & Martí, J. 2007, ApJ, 664, L39
Rolke, W. A., López, A. M., & Conrad, J. 2005, Nucl. Instrum. Method. A, 551, 493
Romero, G. E., et al. 2007, A&A, 474, 15
Sidoli, L., Pellizzoni, A., Vercellone, S., Moroni, M., Mereghetti, S., & Tavani, M. 2006, A&A, 459, 901
Szomoru, A., et al. 2006, Proc. SPIE, 6267, 62673X
Taylor, A. R., et al. 1996, A&A, 305, 817